INTERNATIONAL JOURNAL OF CIRCUIT THEORY AND APPLICATIONS
Int. J. Circ. Theor. Appl. 2008; **36**:473–492
Published online 21 September 2007 in Wiley InterScience (www.interscience.wiley.com). DOI: 10.1002/cta.453

Design equations for fractional-order sinusoidal oscillators: Four practical circuit examples

A. G. Radwan[1], A. M. Soliman[2] and A. S. Elwakil[3,*,†]

[1]*Department of Engineering Mathematics, Faculty of Engineering, Cairo University, Egypt*
[2]*Department of Electronics & Communications, Faculty of Engineering, Cairo University, Egypt*
[3]*Department of Electrical & Computer Engineering, University of Sharjah, Emirates*

SUMMARY

Four practical sinusoidal oscillators are studied in the general form where fractional-order energy storage elements are considered. A fractional-order element is one whose complex impedance is given by $Z = a(\mathrm{j}\omega)^{\pm\alpha}$, where a is a constant and α is not necessarily an integer. As a result, these oscillators are described by sets of fractional-order differential equations. The integer-order oscillation condition and oscillation frequency formulae are verified as special cases. Numerical and PSpice simulation results are given. Experimental results are also reported for a selected Wien-bridge oscillator. Copyright © 2007 John Wiley & Sons, Ltd.

Received 10 October 2006; Revised 8 August 2007; Accepted 14 August 2007

KEY WORDS: fractional calculus; oscillators; fractional-order oscillators; circuit theory

1. INTRODUCTION

Recently, there has been a growing interest in the applications of fractional calculus in various disciplines [1–6]. On the electronic circuits front, the *current–voltage* relationships in the classical inductor and capacitor energy storage elements are governed by first-order differential equations. Hence, any system constructed using n such elements is described by an nth-order system of differential equations. For example, sinusoidal oscillators, which are key electronic building blocks, are classically known to be realizable using at least a second-order circuit. Most of the famous oscillators are either second-order or third-order oscillators. It is evident that available circuit design techniques are dominantly based on the assumption of a target realizable integer-order circuit.

*Correspondence to: A. S. Elwakil, Department of Electrical & Computer Engineering, University of Sharjah, Emirates.
†E-mail: elwakil@ieee.org, elwakil@sharjah.ac.ae

Four decades ago, some researchers investigated the feasibility of approximating a fractional-order capacitor [7, 8]. A finite element approximation of the special case $Z=1/C(j\omega)^{1/2}$ was reported in [9]. This finite element approximation relies on semi-infinite self-similar RC trees. The technique was later developed further by the authors of References [10–12] in order to approximate any $Z=a(j\omega)^{\pm\alpha}$, where α is arbitrary, and the device with such an impedance was termed 'fractance device'. Finite element approximations offer a valuable tool by which the effect of a fractance device can be simulated using a standard circuit simulator or studied experimentally. However, they do not offer a single practical device. Therefore, investigations of fractional-order circuits remained limited and confined mostly to simulations of special case circuits due to the non-existence of a real fractance device and hence the lack of practical motivation [13–15].

Most recently, there has been growing evidence of the possibility of fabricating a real two-terminal fractional capacitor [16, 17]. The fabricated probe described in [16, 17] is based on a metal–insulator–liquid interface and was used in [17] in a fractional-order differentiator circuit. The phase angle between the voltage and current in this capacitor is $\alpha\pi/2$ rather than $\pi/2$ in a normal integer-order capacitor. Although it is not easy to reproduce the device described by the authors as it involves several chemical procedures, with ongoing research and more application motivation, the device may surely become commercially available in the future. Should this happen, circuit designers will be faced with the challenge as to how to utilize the device in constructing their application circuits, particularly as the available design techniques have to be generalized from the narrow integer-order subset to the more general fractional-order domain.

In this paper we study four well-known sinusoidal oscillator circuits, assuming that they are constructed using fractance devices. Two of the studied oscillators (the Wien-bridge oscillator family and the negative resistor oscillator) require two fractance devices, whereas the other two (the Twin-T and Hartley oscillators) require three fractance devices. We show that these famous oscillators can still be designed to oscillate with fractance devices, given that the classical oscillation conditions are modified as mathematically derived in the paper. We also show that fractional-order oscillators have a significant advantage which may be exploited. In particular, the oscillation frequency does not only depend on the values of the reactive elements (L and/or C) but also on their fractional-order α, which adds an extra degree of design freedom. Numerical and PSpice simulation results are shown for all cases. For the PSpice simulations, the finite element approximations reported in [10–12] were used. Also, experimental results of a fractional-order Wien-bridge oscillator whose order varies from approximately 1.6 to 1.9 are reported for the first time.

It is worth noting that linear integer or fractional-order differential equations cannot admit sustained oscillations. To obtain an accurate oscillator model requires the modelling equations to be nonlinear. It is also known that the Barkhausen criterion presents a necessary but not sufficient condition for oscillation. In particular, an oscillator might actually latch-up and never oscillate as intended even if the Barkhausen criterion is satisfied [18]. However, circuit designers still apply the Barkhausen criterion to a linearized around the origin equilibrium point model of their oscillator circuit in order to find the oscillation condition and oscillation frequency. The four selected examples in this paper are known to oscillate and not exhibit latch-up. Hence, to compare the derived formulae with existing integer-order ones, the authors have also considered applying the marginal stability condition (Barkhausen criterion) to the four oscillator models after being modified to represent non-integer-order oscillators. The stability of fractional-order differential equations was studied, for example, in [19–22] and recently in [23] where it was shown that a fractional-order differential equation can be transformed into a polynomial, in

DOI: 10.1002/cta

the so-called W-plane. Locations of the roots of this polynomial are indicators of the system's local stability. It is also worth noting that some fractional-order oscillators were considered by the authors of References [5, 24] and that the fractional-order Fourier transform was considered in [25].

2. BACKGROUND

The Riemann–Liouville definition of a fractional derivative of order α is given by [26, 27]:

$$D^{\alpha} f(t) := \begin{cases} \dfrac{\mathrm{d}^m}{\mathrm{d}t^m}\left[\dfrac{1}{\Gamma(m-\alpha)}\displaystyle\int_0^t \frac{f(\tau)}{(t-\tau)^{\alpha+1-m}}\,\mathrm{d}\tau\right] & (m-1)<\alpha<m \\ \dfrac{\mathrm{d}^m}{\mathrm{d}t^m} f(t) & \alpha = m \end{cases} \tag{1}$$

whereas the Grünwald–Letnikov approximation of a fractional derivative of order α is given by [28]

$$D_t^{\alpha} f(t) \equiv \lim_{\Delta T \to 0} \frac{(\Delta T)^{-\alpha}}{\Gamma(-\alpha)} \sum_{j=0}^{\infty} \frac{\Gamma(\mathrm{j}-\alpha)}{\Gamma(\mathrm{j}+1)} f(t-\mathrm{j}\Delta T) \tag{2}$$

where $\Gamma()$ is the gamma function and ΔT is a discrete time-step. Throughout this work, numerical simulations are performed using the Grünwald–Letnikov approximation.

According to the theorem developed in [29], a linear fractional-order system of the form

$$\begin{pmatrix} D^{\alpha} X_1 \\ D^{\beta} X_2 \end{pmatrix} = \begin{pmatrix} a_{11} & a_{12} \\ a_{21} & a_{22} \end{pmatrix} \begin{pmatrix} X_1 \\ X_2 \end{pmatrix} = AX \tag{3}$$

will oscillate if and only if there exists a value for ω which satisfies simultaneously the following two equations:

$$\begin{aligned} \omega^{\alpha+\beta}\cos(0.5(\alpha+\beta)\pi) - a_{11}\omega^{\beta}\cos(0.5\beta\pi) - a_{22}\omega^{\alpha}\cos(0.5\alpha\pi) + |A| = 0 \\ \omega^{\beta}\sin(0.5(\alpha+\beta)\pi) - a_{11}\omega^{\beta-\alpha}\sin(0.5\beta\pi) - a_{22}\sin(0.5\alpha\pi) = 0 \end{aligned} \tag{4}$$

where $|A|$ is the determinant of the matrix A. The phase difference Φ between the two states $X_1(t)$ and $X_2(t)$ is then found to be

$$\begin{aligned} \Phi &= \Phi_{\alpha} - \frac{\pi(1-\mathrm{sign}(a_{12}))}{2} = \frac{\pi(1-\mathrm{sign}(a_{21}))}{2} - \Phi_{\beta} \\ \Phi_{\alpha} &= \tan^{-1}\frac{\omega^{\alpha}\sin(0.5\alpha\pi)}{\omega^{\alpha}\cos(0.5\alpha\pi) - a_{11}} \quad \text{and} \quad \Phi_{\beta} = \tan^{-1}\frac{\omega^{\beta}\sin(0.5\beta\pi)}{\omega^{\beta}\cos(0.5\beta\pi) - a_{22}} \end{aligned} \tag{5}$$

Table I is a summary of important special cases for such a system. Table II gives two mathematical examples for systems described by Equation (3) with numerical simulation results.

DOI: 10.1002/cta

Table I. Special cases of the fractional-order system described by Equation (3).

No.	Case	Oscillation condition and oscillation frequency (ω)
1	$\alpha=\beta\neq1$	$\mathrm{tr}(A)=a_{11}+a_{22}=2\sqrt{\lvert A\rvert}\cos\left(\frac{\alpha\pi}{2}\right)$ $\omega=\left(\frac{\mathrm{tr}(A)}{2\cos(0.5\alpha\pi)}\right)^{1/\alpha}=(\lvert A\rvert)^{1/2\alpha}$
2	$\alpha=\beta=1$	$\mathrm{tr}(A)=a_{11}+a_{22}=0$ $\omega=\sqrt{\lvert A\rvert}$
3	$\beta=2\alpha$	$\lvert A\rvert=a_{11}p^{2\alpha}\cos(\alpha\pi)+a_{22}p^{\alpha}\cos\left(\frac{\alpha\pi}{2}\right)-p^{3\alpha}\cos\left(\frac{3\alpha\pi}{2}\right)$ $\omega=\left(\frac{a_{11}\cos(0.5\alpha\pi)+\sqrt{a_{11}^2\cos^2(0.5\alpha\pi)+a_{22}(4\cos^2(0.5\alpha\pi)-1)}}{4\cos^2(0.5\alpha\pi)-1}\right)^{1/\alpha}$
4	$\beta=1$ $\alpha=0.5$	$\lvert A\rvert=\sqrt{\frac{\omega}{2}}(a_{22}+\omega)$ $\omega=\frac{a_{11}^2}{2}\left(1+\sqrt{1+\frac{2a_{22}}{a_{11}^2}}\right)^2$
5	$a_{11}=0$	$\lvert A\rvert=\omega^{\alpha}\left(\frac{a_{22}\sin(0.5\beta\pi)}{\sin(0.5(\alpha+\beta)\pi)}\right)$ $\omega=\left(\frac{a_{22}\sin(0.5\alpha\pi)}{\sin(0.5(\alpha+\beta)\pi)}\right)^{1/\beta}$
6	$a_{11}=0$ $a_{22}=0$	$\alpha+\beta=2$ $\omega=\sqrt{\lvert A\rvert}$
7	$\Phi=\frac{\pi}{2}$	$\omega=\left(\frac{a_{11}}{\cos(0.5\alpha\pi)}\right)^{1/\alpha}=\left(\frac{a_{22}}{\cos(0.5\beta\pi)}\right)^{1/\beta}=\left(\frac{\lvert A\rvert}{\cos(0.5(\alpha-\beta)\pi)}\right)^{1/\alpha+\beta}$
8	$a_{12}=0$ or $a_{21}=0$	Impossible to oscillate

DOI: 10.1002/cta

Table II. Two mathematical examples for systems described by Equation (3).

	Example 1	Example 2
ODE	$D^{\alpha+\beta}X - D^{\beta}X + kX = 0$	$D^{\alpha+\beta}X + kX = 0$
State matrix	$\begin{pmatrix} 1 & 1 \\ -k & 0 \end{pmatrix}$	$\begin{pmatrix} 0 & 1 \\ -k & 0 \end{pmatrix}$
Oscillation frequency	$\left(\frac{\sin(0.5\beta\pi)}{\sin(0.5(\alpha+\beta)\pi)}\right)^{1/\alpha}$	$\sqrt{k}$
Oscillation condition	$k = \omega^{\beta}\left(\frac{\sin(0.5\alpha\pi)}{\sin(0.5(\alpha+\beta)\pi)}\right)$	$\alpha+\beta=2$
Φ	$\pi(1-0.5\beta)$	$0.5\alpha\pi = \pi(1-0.5\beta)$
Numerical simulations	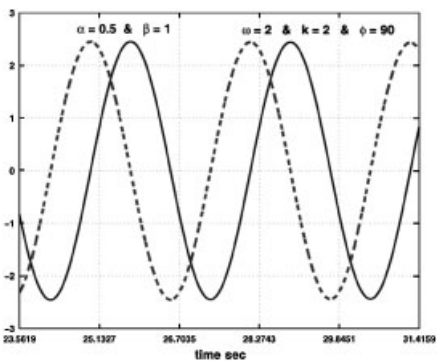	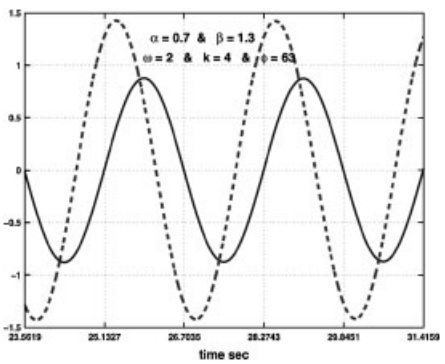

Meanwhile, a linear system with three fractional elements can be described by

$$\begin{pmatrix} D^{\alpha}X_1 \\ D^{\beta}X_2 \\ D^{\gamma}X_3 \end{pmatrix} = \begin{pmatrix} a_{11} & a_{12} & a_{13} \\ a_{21} & a_{22} & a_{23} \\ a_{31} & a_{32} & a_{33} \end{pmatrix} \begin{pmatrix} X_1 \\ X_2 \\ X_3 \end{pmatrix} = AX \tag{6}$$

Using the theorem in [29], this system will oscillate if there exists a value for ω to satisfy simultaneously the following two equations:

$$\begin{aligned} &\omega^{\alpha+\beta+\gamma}\cos(0.5(\alpha+\beta+\gamma)\pi) - a_{22}\omega^{\alpha+\gamma}\cos(0.5(\alpha+\gamma)\pi) - a_{33}\omega^{\alpha+\beta}\cos(0.5(\alpha+\beta)\pi) \\ &- a_{11}\omega^{\beta+\gamma}\cos(0.5(\beta+\gamma)\pi) + \omega^{\alpha}|A_{\alpha}|\cos(0.5\alpha\pi) + \omega^{\beta}|A_{\beta}|\cos(0.5\beta\pi) \\ &+ \omega^{\gamma}|A_{\gamma}|\cos(0.5\gamma\pi) - |A| = 0 \end{aligned} \tag{7a}$$

DOI: 10.1002/cta

Table III. Two mathematical examples for systems described by Equation (6).

	Example 1	Example 2
ODE	$D^{\alpha+\beta+\gamma}X=kX$	$D^{\alpha+\beta+\gamma}X=D^{\alpha}X+kX$
State matrix	$A=\begin{pmatrix}0 & 1 & 0\\ 0 & 0 & 1\\ k & 0 & 0\end{pmatrix}$	$A=\begin{pmatrix}0 & 1 & 0\\ 1 & 0 & 1\\ k & 0 & 0\end{pmatrix}$
Main parameters	$\mathrm{tr}(A)=0$ and $\lvert A\rvert=k$ $\lvert A_\alpha\rvert=\lvert A_\beta\rvert=\lvert A_\gamma\rvert=0$	$\mathrm{tr}(A)=0$ and $\lvert A\rvert=k$ $\lvert A_\alpha\rvert=\lvert A_\beta\rvert=0$ and $\lvert A_\gamma\rvert=-1$
Oscillation frequency	$\omega=\sqrt{(-k)}$	$\omega^{\alpha+\beta}=\dfrac{\sin(0.5\gamma\pi)}{\sin(0.5(\alpha+\beta+\gamma)\pi)}$
Oscillation condition	$\alpha+\beta+\gamma=2$	$k=-\omega^{\gamma}\dfrac{\sin(0.5(\alpha+\beta)\pi)}{\sin(0.5(\alpha+\beta+\gamma)\pi)}$
Numerical simulation	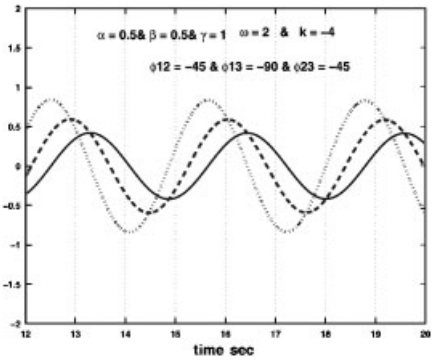	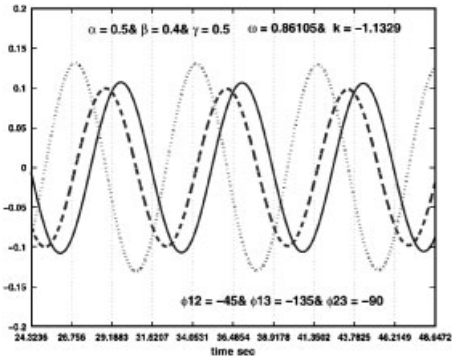

$$\omega^{\alpha+\beta+\gamma}\sin(0.5(\alpha+\beta+\gamma)\pi)-a_{22}\omega^{\alpha+\gamma}\sin(0.5(\alpha+\gamma)\pi)-a_{33}\omega^{\alpha+\beta}\sin(0.5(\alpha+\beta)\pi)$$
$$-a_{11}\omega^{\beta+\gamma}\sin(0.5(\beta+\gamma)\pi)+\omega^{\alpha}|A_\alpha|\sin(0.5\alpha\pi)+\omega^{\beta}|A_\beta|\sin(0.5\beta\pi)$$
$$+\omega^{\gamma}|A_\gamma|\sin(0.5\gamma\pi)=0 \tag{7b}$$

where $|A|$ is the determinant of the matrix A,

$$|A_\alpha|=\begin{vmatrix}a_{22} & a_{23}\\ a_{32} & a_{33}\end{vmatrix},\quad |A_\beta|=\begin{vmatrix}a_{11} & a_{13}\\ a_{31} & a_{33}\end{vmatrix}\quad\text{and}\quad |A_\gamma|=\begin{vmatrix}a_{11} & a_{12}\\ a_{21} & a_{22}\end{vmatrix}$$

Table III shows two examples of systems described by Equation (6).

In the following circuit simulations, a fractional-order capacitor $Y_{C_F}=C_F s^{0.5}$ is approximated using the finite element circuit reported in [10] and is shown in Figure 1(a) with $C_F=\sqrt{C/R}$. To realize any other fractional-order $\alpha<1$, the finite element approximation of [12], shown in

DOI: 10.1002/cta

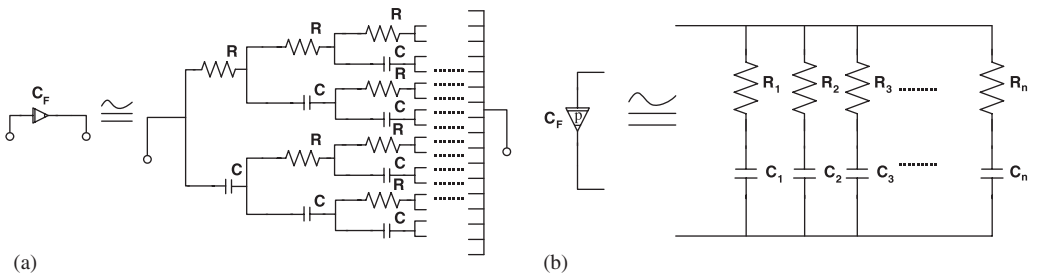

Figure 1. (a) Finite element approximation of a fractal capacitor of order 0.5 and (b) approximation of a fractal capacitor of any order $\alpha<1$.

Figure 1(b), is used. For example, to approximate $Y_{C_F}=(37.1\,\mu\text{F})s^{0.4}$ requires $n=31$ branches with $R_{k+1}/R_k=0.569$ and $C_{k+1}/C_k=0.429$ [12].

3. OSCILLATORS WITH TWO FRACTIONAL CAPACITORS

3.1. Fractional-order Wien oscillators

The fractional-order Wien oscillators shown in Figure 2 can all be modelled by Equation (3) around the equilibrium point at the origin. The design procedure for all members of this family is similar and may be demonstrated on the circuit of Figure 2(a), which is modelled (taking the nonlinear behavior of the op amp into account) by

$$\begin{pmatrix} \dfrac{\mathrm{d}^{\alpha}V_{C_1}}{\mathrm{d}t^{\alpha}} \\ \dfrac{\mathrm{d}^{\beta}V_{C_2}}{\mathrm{d}t^{\beta}} \end{pmatrix} = \begin{pmatrix} \dfrac{-1}{R_1C_1} & \dfrac{a}{R_1C_1} \\ \dfrac{-1}{R_1C_2} & \dfrac{a}{R_1C_2}-\dfrac{1}{R_2C_2} \end{pmatrix} \begin{pmatrix} V_{C_1} \\ V_{C_2} \end{pmatrix} + \begin{pmatrix} \dfrac{b}{R_1C_1} \\ \dfrac{b}{R_1C_2} \end{pmatrix} \tag{8a}$$

$$(a,b)=\begin{cases} (-1,V_{\text{sat}}), & \left(1+\dfrac{R_3}{R_4}\right)V_{C_2}\geqslant V_{\text{sat}} \\ \left(\dfrac{R_3}{R_4},0\right), & -V_{\text{sat}}<\left(1+\dfrac{R_3}{R_4}\right)V_{C_2}<V_{\text{sat}} \\ (-1,-V_{\text{sat}}), & -V_{\text{sat}}\geqslant\left(1+\dfrac{R_3}{R_4}\right)V_{C_2} \end{cases} \tag{8b}$$

where V_{sat} is the op amp saturation voltage, α and β are the fractional orders of the two capacitors (see Figure 2(a)). Using Equation (4), we may solve for the design parameter $a=R_3/R_4$

DOI: 10.1002/cta

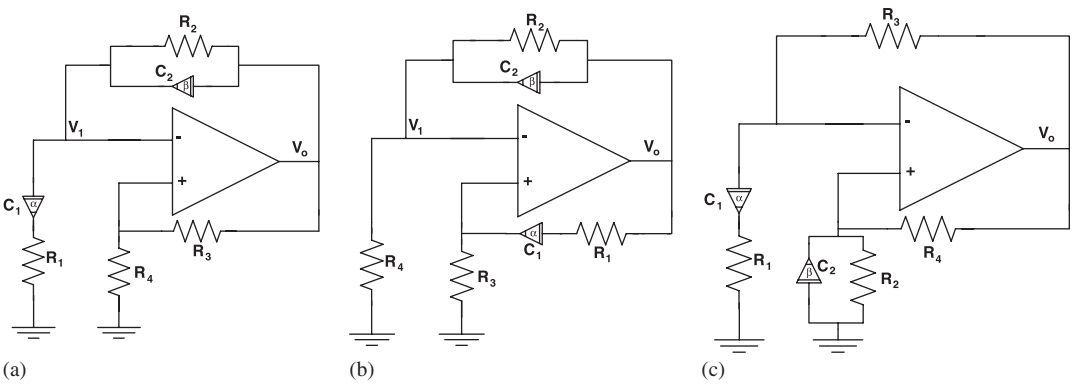

Figure 2. Fractional-order Wien oscillators with two fractional capacitors.

(note that the op amp is employed as an amplifier whose gain $k=1+a$) to obtain

$$a=\frac{R_1R_2C_1C_2\omega^{\alpha+\beta}\cos(0.5(\alpha+\beta)\pi)+R_2C_2\omega^{\beta}\cos(0.5\beta\pi)+R_1C_1\omega^{\alpha}\cos(0.5\alpha\pi)+1}{R_2C_1\omega^{\alpha}\cos(0.5\alpha\pi)}$$
$$=\frac{R_1R_2C_1C_2\omega^{\alpha+\beta}\sin(0.5(\alpha+\beta)\pi)+R_2C_2\omega^{\beta}\sin(0.5\beta\pi)+R_1C_1\omega^{\alpha}\sin(0.5\alpha\pi)}{R_2C_1\omega^{\alpha}\sin(0.5\alpha\pi)} \tag{9}$$

Equating both sides of Equation (9) gives the oscillation frequency as the solution to the following equation:

$$R_1R_2C_1C_2\omega^{\alpha+\beta}\sin(0.5\beta\pi)+R_2C_2\omega^{\beta}\sin(0.5(\beta-\alpha)\pi)-\sin(0.5\alpha\pi)=0 \tag{10}$$

Note that ω does not only depend on the component values but also on α and β, which gives two extra degrees of freedom in the design process. The design steps for this oscillator are as follows: given R_1, R_2, C_1, C_2, α and β, Equation (10) is solved to obtain the frequency of oscillation ω and then the necessary value of $a=R_3/R_4$ can be obtained from Equation (9). Table IV is a summary of some special cases for this oscillator. The design equations of the second row of the table are those of the well-known second-order case.

Note that a simplified design procedure may be followed if we define $1/R_1C_1=\lambda^{\beta}$, $1/R_1R_2C_1C_2=\lambda^{\alpha+\beta}$ and $\rho=\omega/\lambda$. Equation (10) then becomes

$$\rho^{\alpha+\beta}\sin\left(\frac{\beta\pi}{2}\right)+\rho^{\beta}\sin\left((\beta-\alpha)\frac{\pi}{2}\right)-\sin\left(\frac{\alpha\pi}{2}\right)=0 \tag{11}$$

The design steps are then as follows:

(1) Given the values of α and β, Equation (11) can be solved for ρ.
(2) By selecting values of R_1, C_1 and C_2, R_2 can be obtained as $R_2=(1/C_2)(R_1C_1)^{\beta/\alpha}$.

DOI: 10.1002/cta

Table IV. Special cases for the Wien oscillator of Figure 2(a).

	$a=R_3/R_4$	ω	Φ_α
$\alpha=\beta\neq 1$	$\frac{C_2}{C_1}+\frac{R_1}{R_2}+2\sqrt{\frac{R_1C_2}{R_2C_1}}\cos(0.5\alpha\pi)$	$\left(\frac{1}{R_1R_2C_1C_2}\right)^{1/2\alpha}$	$\tan^{-1}\frac{\sqrt{R_1C_1}\sin(0.5\alpha\pi)}{\sqrt{R_1C_1}\cos(0.5\alpha\pi)+\sqrt{R_2C_2}}$
$\alpha=\beta=1$	$\frac{C_2}{C_1}+\frac{R_1}{R_2}$	$\frac{1}{R_1R_2C_1C_2}$	$\tan^{-1}\sqrt{\frac{R_1C_1}{R_2C_2}}$
$\alpha=\beta\neq 1$ $R_1=R_2=R$ $C_1=C_2=C$	$2(1+\cos(0.5\alpha\pi))$	$\left(\frac{1}{RC}\right)^{1/\alpha}$	$0.25\alpha\pi$
$\alpha=\beta=1$ $R_1=R_2=R$ $C_1=C_2=C$	2	$\frac{1}{RC}$	0.25π

(3) The oscillation frequency is $\omega=\rho(1/R_1C_1)^{1/\alpha}=\rho(1/R_1R_2C_1C_2)^{1/\alpha+\beta}$.
(4) The oscillation condition can be obtained using Equation (9).

The reason why this procedure may be considered simplified is that using Equation (11), a look-up table can be constructed to directly give ρ for any given α and β. Figure 3(a)–(d) shows numerical simulations and the corresponding PSpice simulation results for the two cases $(\alpha,\beta)=(0.4,1)$ and $(0.5,0.5)$, respectively.

3.2. Negative resistor RC oscillator

An RC oscillator that employs the op amp as a negative resistor ($R_{\text{neg}}=-R_3R/R_4$) is shown in Figure 4(a). This oscillator may be modelled in the op amp linear region by

$$\begin{pmatrix}\dfrac{\mathrm{d}^\alpha V_{C_1}}{\mathrm{d}t^\alpha}\\[2ex]\dfrac{\mathrm{d}^\beta V_{C_2}}{\mathrm{d}t^\beta}\end{pmatrix}=\begin{pmatrix}\dfrac{-1}{C_1R_1}\left(1+\dfrac{R_1}{R_2}\right) & \dfrac{1}{R_1C_1}\\[2ex]\dfrac{-1}{R_2C_2}\left(1+\dfrac{R_4}{R_3}\left(1+\dfrac{R_2}{R_1}\right)\right) & \dfrac{R_4}{R_3C_2R}\left(1+\dfrac{R}{R_1}\right)\end{pmatrix}\begin{pmatrix}V_{C_1}\\V_{C_2}\end{pmatrix} \tag{12}$$

from which it is seen that

$$|A|=\frac{1}{R_1R_2C_1C_2}\left(1-\frac{R_4}{RR_3}(R_1+R_2)\right)$$

can be positive or negative, but for stability $|A|$ must remain positive [23].

DOI: 10.1002/cta

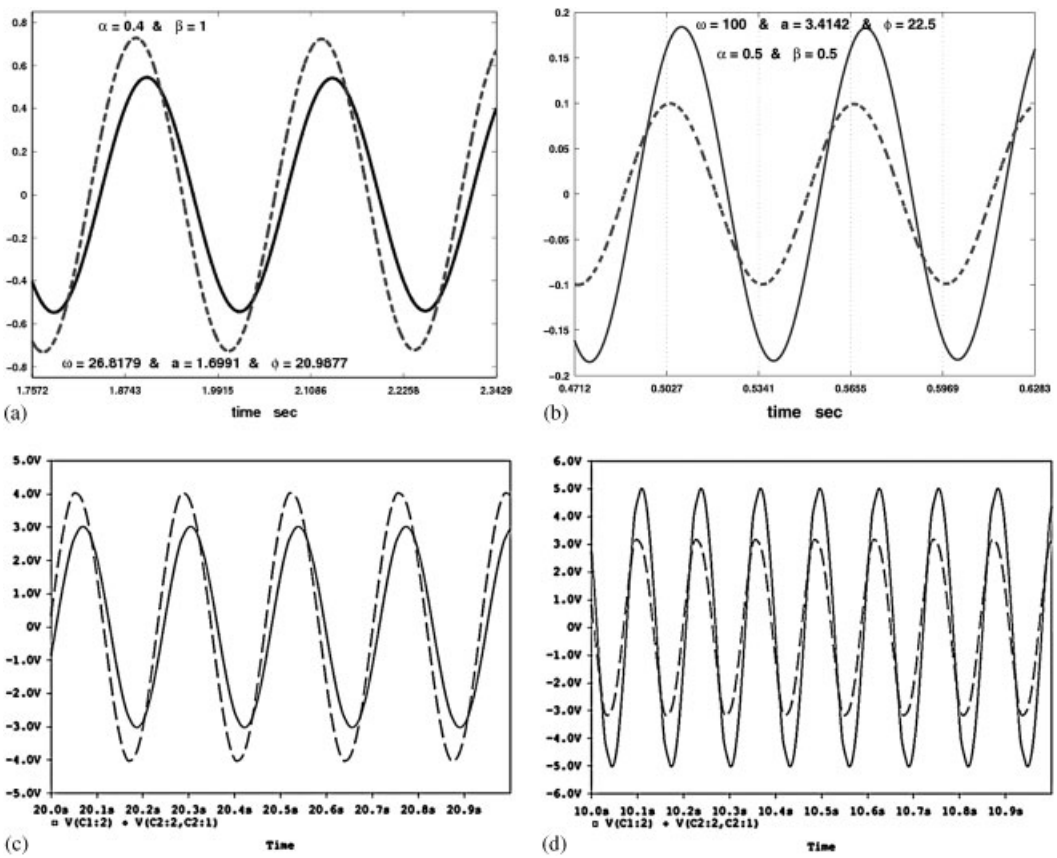

Figure 3. Numerical and PSpice simulations for the Wien oscillator of Figure 2(a) when $R_1 = R_2 = 10\,\text{k}\Omega$ and (a), (c) $\alpha = 0.4$, $\beta = 1$, $a = 1.7$, $C_1 = 37.1\,\mu\text{F}$, $C_2 = 1\,\mu\text{F}$ and (b), (d) $\alpha = \beta = 0.5$, $a = 3.42$, $C_1 = C_2 = 10\,\mu\text{F}$.

Using Equation (4) and assuming that this oscillator's design parameter is the resistance R, the following condition for oscillation is obtained:

$$R = \frac{\dfrac{R_4}{R_3 C_2}\omega^{\alpha}\sin(0.5\alpha\pi)}{\omega^{\alpha+\beta}\sin(0.5(\alpha+\beta)\pi) + \dfrac{(R_1+R_2)\omega^{\beta}\sin(0.5\beta\pi)}{R_1 R_2 C_1} - \dfrac{R_4\omega^{\alpha}\sin(0.5\alpha\pi)}{R_1 R_3 C_2}}$$

$$= \frac{\dfrac{R_4}{R_3 C_2}\left(\omega^{\alpha}\cos(0.5\alpha\pi) + \dfrac{R_1+R_2}{R_1 R_2 C_1}\right)}{\omega^{\alpha+\beta}\cos(0.5(\alpha+\beta)\pi) + \dfrac{(R_1+R_2)\omega^{\beta}\cos(0.5\beta\pi)}{R_1 R_2 C_1} - \dfrac{R_4\omega^{\alpha}\cos(0.5\alpha\pi)}{R_1 R_3 C_2} + \dfrac{1}{R_1 R_2 C_1 C_2}} \tag{13}$$

DOI: 10.1002/cta

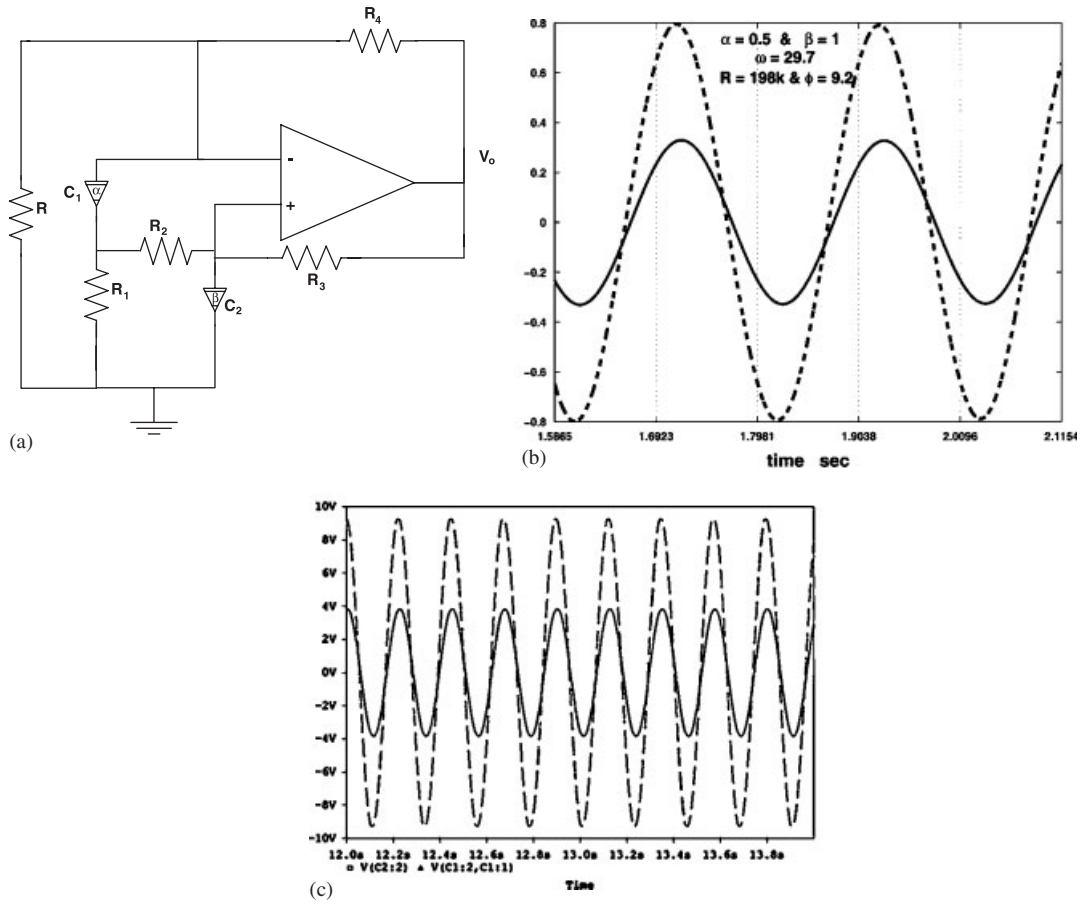

Figure 4. (a) Negative resistor oscillator circuit and (b), (c) numerical and PSpice simulations for $\alpha=0.5$, $\beta=1$, $R_1=R_2=10\,\text{k}\Omega$, $R_3=4\,\text{k}\Omega$, $R_4=7\,\text{k}\Omega$, $R=198\,\text{k}\Omega$, $C_1=10\,\mu\text{F}$ and $C_2=1\,\mu\text{F}$.

Equating the two sides of (13) yields the oscillation frequency as the solution of

$$\omega^{\alpha+\beta}\sin(0.5\beta\pi)+\frac{2\omega^{\beta}(R_1+R_2)}{R_1R_2C_1}\sin(0.5\beta\pi)\cos(0.5\alpha\pi)$$

$$+\omega^{\beta-\alpha}\left(\frac{R_1+R_2}{R_1R_2C_1}\right)^2\sin(0.5\beta\pi)-\frac{\sin(0.5\alpha\pi)}{R_1R_2C_1C_2}\left(1+\frac{R_4}{R_3}\left(1+\frac{R_2}{R_1}\right)\right)=0 \qquad (14)$$

Similar design steps as for the Wien oscillator family (Section 3.1) can subsequently be followed. Table V summarizes some special cases for this RC oscillator. The design equations of the

DOI: 10.1002/cta

Table V. Special cases of the RC oscillator of Figure 4(a).

Cases	Oscillation frequency, oscillation condition and stability condition
	$\omega^{2\alpha}+2\omega^{\alpha}\left(\frac{R_1+R_2}{R_1R_2C_1}\right)\cos\left(\frac{\alpha\pi}{2}\right)+\left(\frac{R_1+R_2}{R_1R_2C_1}\right)^2-\frac{(R_1R_3+R_4(R_1+R_2))}{R_1^2R_2R_3C_1C_2}=0$
$\alpha=\beta<1$	$R=\frac{R_1R_2C_1R_4}{2R_1R_2R_3C_1C_2\omega^{\alpha}\cos(0.5\alpha\pi)+R_3C_2(R_1+R_2)-R_2C_1R_4}$
	(for stability) $\left(1+\frac{R_2}{R_1}\right)\frac{C_2}{C_1}\geqslant\frac{R_4}{R_3}>\left(1+\frac{R_2}{R_1}\right)\frac{C_2}{C_1}-\frac{R_1}{R_1+R_2}$
	$\omega=\sqrt{\left(\frac{1}{R_1R_2C_1C_2}\left(1+\frac{R_4}{R_3}\left(1+\frac{R_2}{R_1}\right)\right)-\left(\frac{R_1+R_2}{R_1R_2C_1}\right)^2\right)}$
$\alpha=\beta=1$	$R=\frac{R_1R_4R_2C_1}{(R_1+R_2)R_3C_2-R_4R_2C_1}$
	(for stability) $\left(1+\frac{R_2}{R_1}\right)\frac{C_2}{C_1}\geqslant\frac{R_4}{R_3}>\left(1+\frac{R_2}{R_1}\right)\frac{C_2}{C_1}-\frac{R_1}{R_1+R_2}$
$\alpha=\beta$ and $R_1=R_2=R_3=R_4=R_e$ $C_1=C_2=C$	$R_e^2C^2\omega^{2\alpha}+4R_eC\omega^{\alpha}\cos(0.5\alpha\pi)+1=0$ $R=\frac{R_e}{2CR_e\omega^{\alpha}\cos(0.5\alpha\pi)+1}$ (for stability) $\alpha>\frac{4}{3}$
$\alpha=\beta$ and $R_1=R_2=R_3=R_4=R_e$	$\omega^{2\alpha}+\left(\frac{4\omega^{\alpha}}{R_eC_1}\right)\cos\left(\frac{\alpha\pi}{2}\right)+\left(\frac{1}{R_eC}\right)^2\left(4-\frac{3C_1}{C_2}\right)=0$ $R=\frac{R_eC_1}{2R_eC_1C_2\omega^{\alpha}\cos(0.5\alpha\pi)+2C_2-C_1}$ (for stability) $2\geqslant\frac{C_1}{C_2}>\frac{4}{3}$

second row of the table are those of the well-known second-order case. Numerical and PSpice simulations for this oscillator are shown in Figure 4(b) and (c) when $R_1=10\,\mathrm{k}\Omega$, $\alpha=0.5$ and $\beta=1$.

DOI: 10.1002/cta

4. OSCILLATORS WITH THREE FRACTIONAL ELEMENTS

4.1. Twin-T oscillator

Figure 5(a) and (b) shows the fractional Twin-T oscillator circuit, which contains three fractional-order capacitors of orders α, β and γ. The oscillator is described by

$$\begin{pmatrix} \frac{\mathrm{d}^{\alpha}V_{C_1}}{\mathrm{d}t^{\alpha}} \\ \frac{\mathrm{d}^{\beta}V_{C_2}}{\mathrm{d}t^{\beta}} \\ \frac{\mathrm{d}^{\gamma}V_{C_3}}{\mathrm{d}t^{\gamma}} \end{pmatrix} = \begin{pmatrix} \frac{1}{aC_1}\left(\frac{1}{R_2}+\frac{1}{R_3}\right) & \frac{-1}{aC_1}\left(\frac{1}{R_2}+\frac{a+1}{R_3}\right) & \frac{-1}{R_2C_1} \\ \frac{-1}{aR_2C_2} & \frac{1}{aR_2C_2} & \frac{1}{R_2C_2} \\ \frac{1}{aC_3}\left(\frac{a+1}{R_1}+\frac{1}{R_2}\right) & \frac{-1}{aC_3}\left(\frac{a+1}{R_1}+\frac{1}{R_2}\right) & \frac{-1}{C_3}\left(\frac{1}{R_1}+\frac{1}{R_2}\right) \end{pmatrix} \begin{pmatrix} V_{C_1} \\ V_{C_2} \\ V_{C_3} \end{pmatrix} + \begin{pmatrix} \frac{b}{C_1}\left(\frac{1}{R_2}+\frac{1}{R_3}\right) \\ \frac{-b}{R_2C_2} \\ \frac{b}{C_3}\left(\frac{1}{R_1}+\frac{1}{R_2}\right) \end{pmatrix} \tag{15a}$$

where

$$(a,b)=\begin{cases} (-1, V_{\mathrm{sat}}), & \dfrac{-k}{k+1}(V_{C_1}-V_{C_2}) \geqslant V_{\mathrm{sat}} \\ (k,0), & -V_{\mathrm{sat}} < \dfrac{-k}{k+1}(V_{C_1}-V_{C_2}) < V_{\mathrm{sat}} \\ (-1,-V_{\mathrm{sat}}), & -V_{\mathrm{sat}} \geqslant \dfrac{-k}{k+1}(V_{C_1}-V_{C_2}) \geqslant V_{\mathrm{sat}} \end{cases} \tag{15b}$$

Defining the following parameters

$$\begin{aligned} &a_{11}=\frac{p_{11}}{k}, \quad |A_{\alpha}|=\frac{1}{R_1R_2C_2C_3}=p_{\alpha}, \quad a_{22}=\frac{p_{22}}{k} \\ &a_{33}=-p_{33} \quad \text{and} \quad |A|=\frac{-1}{R_1R_2R_3C_1C_2C_3}=-p_d \\ &|A_{\beta}|=\frac{1}{R_1R_2C_1C_3}-\frac{1}{kR_1R_3C_1C_3}\left(1+\frac{R_1}{R_2}\right)=p_{\beta f}-\frac{p_{\beta e}}{k} \quad \text{and} \\ &|A_{\gamma}|=\frac{-1}{kR_2R_3C_1C_2}=\frac{-p_{\gamma}}{k} \end{aligned} \tag{16}$$

DOI: 10.1002/cta

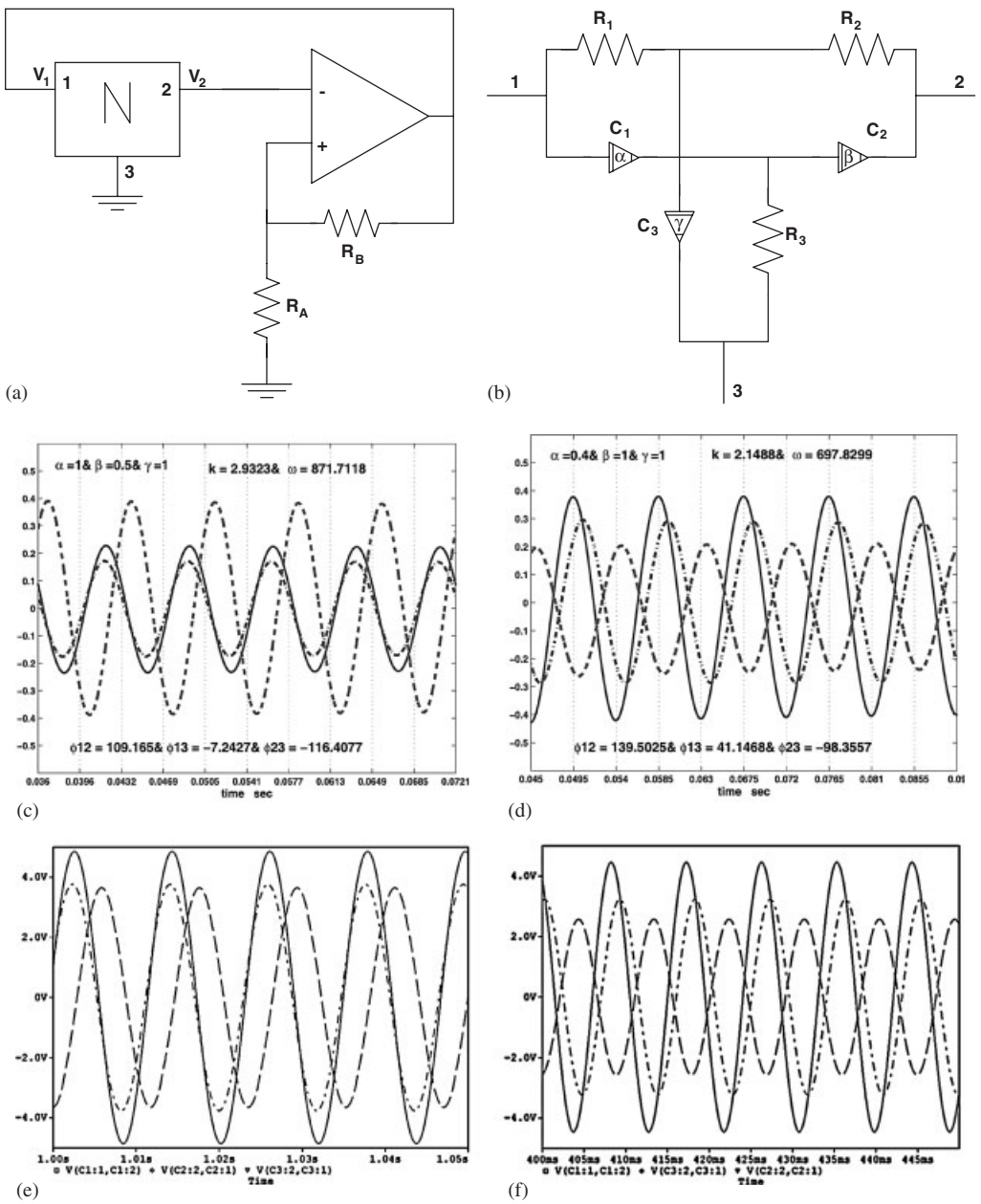

Figure 5. (a) The Twin-T oscillator structure; (b) fractional-order Twin-T network; (c)–(f) numerical and PSpice simulations with $R_1 = 10\,\text{k}\Omega$, $R_2 = 1\,\text{k}\Omega$, $R_3 = 5\,\text{k}\Omega$; (c), (e) $\alpha = \gamma = 1$, $\beta = 0.5$, $C_1 = C_3 = 1\,\mu\text{F}$, $C_2 = 10\,\mu\text{F}$ and (d), (f) $\beta = \gamma = 1$, $\alpha = 0.4$, $C_2 = C_3 = 1\,\mu\text{F}$, $C_1 = 37.1\,\mu\text{F}$.

DOI: 10.1002/cta

where k is the amplifier gain, and substituting it into Equation (9), the oscillation condition is found to be

$$k = \frac{p_{22}\omega^{\alpha+\gamma}\sin(0.5(\alpha+\gamma)\pi)+p_{11}\omega^{\beta+\gamma}\sin(0.5(\beta+\gamma)\pi)+p_{\beta e}\omega^{\beta}\sin(0.5\beta\pi)+p_{\gamma}\omega^{\gamma}\sin(0.5\gamma\pi)}{\omega^{\alpha+\beta+\gamma}\sin(0.5(\alpha+\beta+\gamma)\pi)+p_{33}\omega^{\alpha+\beta}\sin(0.5(\alpha+\beta)\pi)+p_{\alpha}\omega^{\alpha}\sin(0.5\alpha\pi)+p_{\beta f}\omega^{\beta}\sin(0.5\beta\pi)}$$

$$= \frac{p_{22}\omega^{\alpha+\gamma}\cos(0.5(\alpha+\gamma)\pi)+p_{11}\omega^{\beta+\gamma}\cos(0.5(\beta+\gamma)\pi)+p_{\beta e}\omega^{\beta}\cos(0.5\beta\pi)+p_{\gamma}\omega^{\gamma}\cos(0.5\gamma\pi)}{\omega^{\alpha+\beta+\gamma}\cos(0.5(\alpha+\beta+\gamma)\pi)+p_{33}\omega^{\alpha+\beta}\cos(0.5(\alpha+\beta)\pi)+p_{\alpha}\omega^{\alpha}\cos(0.5\alpha\pi)+p_{\beta f}\omega^{\beta}\cos(0.5\beta\pi)+p_{d}} \quad (17)$$

By equating the two sides of Equation (17), the oscillation frequency can be obtained, as summarized in Table VI for some special cases. The design equations of the fourth row of the table are those of the classical equal-R equal-C third-order case. Figure 5(e)–(h) shows numerical and PSpice simulations of two different cases for this oscillator.

4.2. Hartley oscillator

Figure 6(a) and (b) shows a fractional-order Hartley oscillator and its small signal model. Note here that one fractional capacitor of order α and two fractional inductors of orders β and γ are, respectively, used. The linearized, with respect to the origin state space, small signal model is given by

$$\begin{pmatrix} \dfrac{\mathrm{d}^{\alpha}V_C}{\mathrm{d}t^{\alpha}} \\ \dfrac{\mathrm{d}^{\beta}I_{L_1}}{\mathrm{d}t^{\beta}} \\ \dfrac{\mathrm{d}^{\gamma}I_{L_2}}{\mathrm{d}t^{\gamma}} \end{pmatrix} = \begin{pmatrix} 0 & 0 & \dfrac{1}{C} \\ \dfrac{g_m R}{L_1(1+g_m R)} & \dfrac{-R}{L_1(1+g_m R)} & \dfrac{-R}{L_1(1+g_m R)} \\ \dfrac{-1}{L_2(1+g_m R)} & \dfrac{-R}{L_2(1+g_m R)} & \dfrac{-R}{L_2(1+g_m R)} \end{pmatrix} \begin{pmatrix} V_C \\ I_{L_1} \\ I_{L_2} \end{pmatrix} \quad (18)$$

Using Equations (7a) and (7b) and noting that

$$|A_{\alpha}|=0, \quad |A_{\beta}|=\frac{1}{L_2C(1+g_m R)}, \quad |A_{\gamma}|=0, \quad |A|=\frac{-R}{L_1L_2C(1+g_m R)}$$

yield the oscillation condition as

$$(1+g_m R) = -\frac{L_2CR\omega^{\alpha+\gamma-\beta}\sin(0.5(\alpha+\gamma)\pi)+L_1CR\omega^{\alpha}\sin(0.5(\alpha+\beta)\pi)+L_1\sin(0.5\beta\pi)}{L_1L_2C\omega^{\alpha+\gamma}\sin(0.5(\alpha+\beta+\gamma)\pi)}$$

$$= -\frac{L_2CR\omega^{\alpha+\gamma}\cos(0.5(\alpha+\gamma)\pi)+L_1CR\omega^{\alpha+\beta}\cos(0.5(\alpha+\beta)\pi)+L_1\omega^{\beta}\cos(0.5\beta\pi)+R}{L_1L_2C\omega^{\alpha+\beta+\gamma}\cos(0.5(\alpha+\beta+\gamma)\pi)} \quad (19)$$

The oscillation frequency is then the solution to the equation

$$RL_2C\omega^{\alpha+\gamma}\sin(0.5\beta\pi)+RL_1C\omega^{\alpha+\beta}\sin(0.5\gamma\pi)+L_1\omega^{\beta}\sin(0.5(\alpha+\gamma)\pi)$$

$$+R\sin(0.5(\alpha+\beta+\gamma)\pi)=0 \quad (20)$$

DOI: 10.1002/cta

Table VI. Special cases of the twin-T oscillator.

Case a, b, c	Oscillation frequency and oscillation condition
$\alpha=\beta=\gamma$	$a\omega^{4\alpha}+2\omega^{3\alpha}b\cos\left(\frac{\alpha\pi}{2}\right)-2a\omega^{\alpha}p_d\cos\left(\frac{\alpha\pi}{2}\right)-c\omega^{2\alpha}-p_d(p_{\beta e}+p_{\gamma})=0$ $k=\frac{2a\omega^{\alpha}\cos(0.5\alpha\pi)+b}{\omega^{2\alpha}(4\cos^2(0.5\alpha\pi)-1)+2p_{33}\omega^{\alpha}\cos(0.5\alpha\pi)+(p_{\beta f}+p_{\alpha})}$
$\alpha=\beta=\gamma=1$	$\omega=\sqrt{\frac{c+\sqrt{c^2+4abp_d}}{2a}}$ $k=-\frac{a\omega^2}{p_d-p_{33}\omega^2}=\frac{b}{(p_{\beta f}+p_{\alpha})-\omega^2}$
$\alpha=\beta=\gamma$, $C_1=C_2=C_3=C$ $R_1=R_2=R_3=R$	$\omega=\left(\frac{1}{RC}\right)^{1/\alpha}$ $k=\frac{3}{2\cos(0.5\alpha\pi)+1}$
$\alpha=\beta=\gamma=1$ $C_1=C_2=C_3=C$ $R_1=R_2=R_3=R$	$\omega=\frac{1}{RC}$ $k=3$
$\alpha=\beta=\gamma=1$ $k\to\infty$	$\omega=\sqrt{(p_{\alpha}+p_{\beta f})}=\sqrt{\frac{p_d}{p_{33}}}=\frac{1}{\sqrt{C_1C_2R_3(R_1+R_2)}}$ $\frac{R_1R_2}{R_3(R_1+R_2)}=\frac{C_1+C_2}{C_3}$

Note: $a=\frac{1}{C_1R_2}+\frac{1}{C_1R_3}+\frac{1}{C_2R_2}$ and $b=\frac{1}{C_1C_3R_1R_3}+\frac{1}{C_1C_3R_2R_3}+\frac{1}{C_1C_2R_2R_3}$

$c=\frac{1}{C_1C_2C_3R_1R_2R_3}\left(\frac{C_2}{C_3}\left(\frac{R_2}{R_1}+2+\frac{R_1}{R_2}\right)\right)-\frac{C_1R_3}{C_2R_2}-\frac{C_2}{C_1}\left(\frac{R_3}{R_2}+1\right)+\frac{R_1-2R_3}{R_2}$

which is obtained by equating the two sides of Equation (19). Two important special cases can be noted:

(i) if $\alpha=\beta=\gamma$, then Equations (19) and (20) simplify to

$$(1+g_mR)=-\frac{2CR\omega^{\alpha}\cos(0.5\alpha\pi)(L_2+L_1)+L_1}{L_1L_2C\omega^{2\alpha}(4\cos^2(0.5\alpha\pi)-1)} \tag{21}$$

and

$$RC(L_2+L_1)\omega^{2\alpha}+2L_1\cos\left(\frac{\alpha\pi}{2}\right)\omega^{\alpha}+R\left(4\cos^2\left(\frac{\alpha\pi}{2}\right)-1\right)=0 \tag{22}$$

DOI: 10.1002/cta

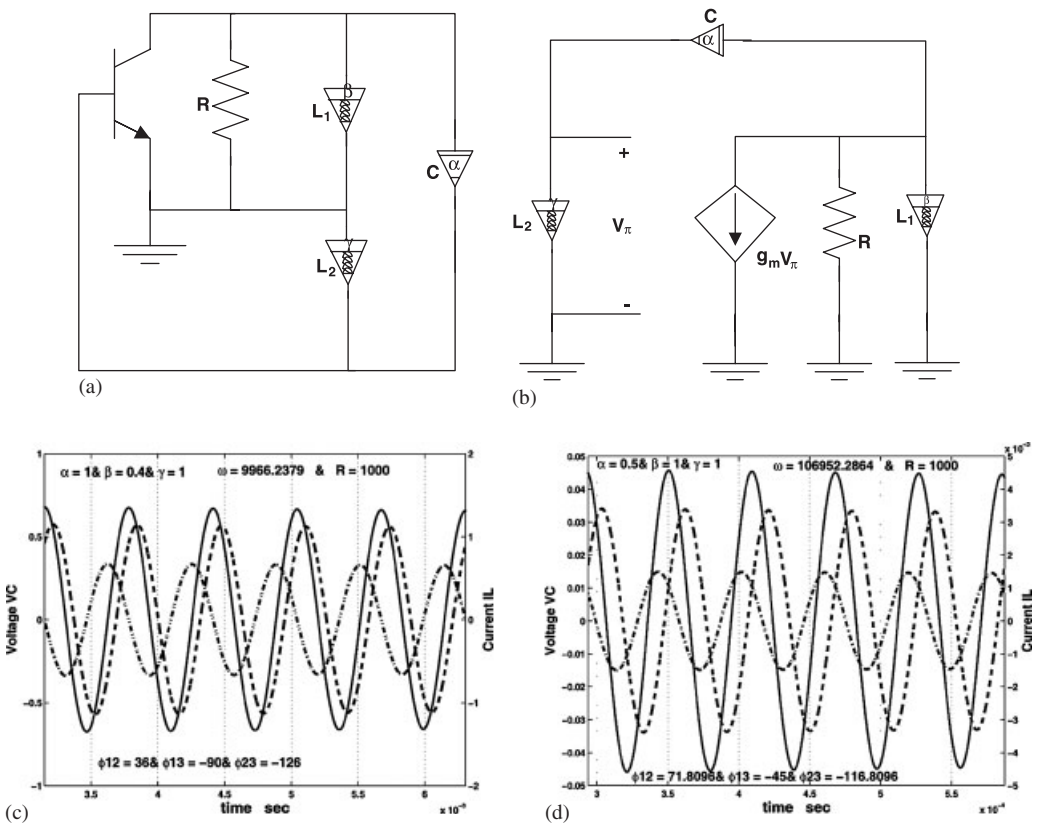

Figure 6. (a) Hartley oscillator and (b) its small signal model. Numerical simulations with $R=1\,\text{k}\Omega$, $L_1=L_2=0.0001\,\text{H}$, $C=100\,\mu\text{F}$ and (c) $\alpha=\gamma=1$, $\beta=0.4$, $C_1=C_3=1\,\mu\text{F}$, $C_2=37.1\,\mu\text{F}$ and (d) $\beta=\gamma=1$, $\alpha=0.5$, $C_2=C_3=1\,\mu\text{F}$, $C_1=10\,\mu\text{F}$.

(ii) if $\alpha=\beta=\gamma=1$ (classical third-order oscillator), Equations (21) and (22) reduce to the famous formulae $\omega=1/\sqrt{C(L_2+L_1)}$ and $g_m R=L_1/L_2$. Figure 6(c) and (d) is the numerical simulation for two different parameter sets of this oscillator.

5. EXPERIMENTAL RESULTS

We have constructed the Wien oscillator, Figure 2(a), using one fractional capacitor donated by Biswas *et al.* [17]. A picture of this capacitive probe is shown in Figure 7(a). A normal capacitor ($\alpha=1$) was used in place of C_1 (see Figure 2(a)), whereas fractional capacitor (of order β), dipped in 1 cm of tab water was used in place of C_2. C_2 was measured to be 3.4 nF; hence, C_1 was also selected to be 3.4 nF. R_1 and R_2 were kept equal. Table VII summarizes the measured frequency (f_{measured}) corresponding to each value of $R=R_1=R_2$. Also shown in the table is the oscillation frequency $f_{RC}=1/2\pi RC$ in each case which is the normal oscillation frequency if the two capacitors were both of integer order. It is clear from the table that $\omega_{\text{measured}}=(\omega_{RC})^{2/(\alpha+\beta)}$

DOI: 10.1002/cta

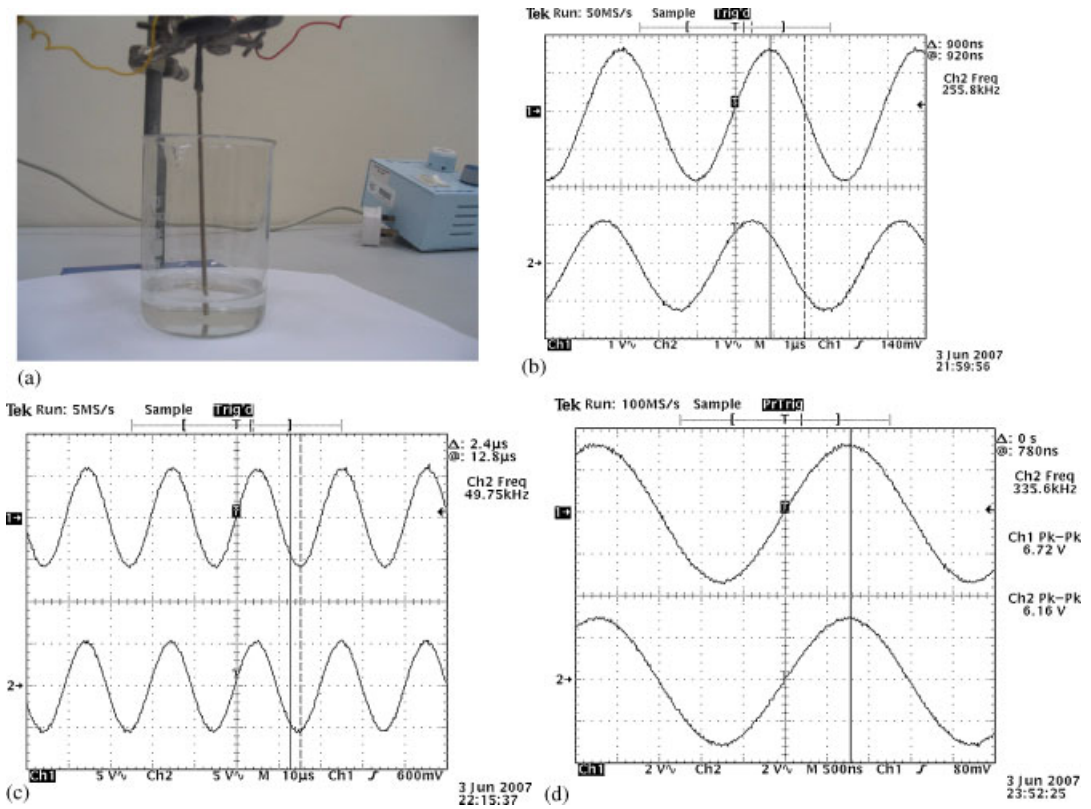

Figure 7. Experimental results of the Wien oscillator in Figure 2(a) using the fractional capacitor (a) dipped in 1 cm of water.

is much larger than ω_{RC} since β is less than one. The fractional-order β is also shown in the table. As R is increased from 0.2 to 30 kΩ, f_{RC} decreases from 23.4 to 1.47 kHz, while β steadily decreases from 0.988 (very close to being an integer-order capacitor) to 0.259. Meanwhile, f_{measured} steadily decreases from 256 to 50 kHz at $R=8$ kΩ. From $R=8$ to 10 kΩ, f_{measured} remains near its minimum of 50 kHz. At $R=11$ kΩ, f_{measured} starts increasing again to reach 318.5 kHz at $R=30$ kΩ. Note that the effective order of this Wien oscillator equals $\alpha+\beta=(1+\beta)<2$. Figure 7(b)–(d) shows the observed oscilloscope waveforms at $R=0.2$, 8 and 20 kΩ, respectively. The two waveforms shown in each figure correspond to the voltages at the two terminals of C_1. In a second-order Wien oscillator, the phase shift Φ between these two waveforms is 45°, whereas in the fractional-order oscillator Φ is as shown in Table VII where it clearly decreases with β. For $\beta<0.5$, Φ is hardly measurable. The measurements were repeated with the fractional capacitor dipped in 2 cm of water. In this case, C_2 was measured to be 6 nF and C_1 was set equal to this value. The results are also summarized in Table VII where it is seen that f_{measured} is far higher than f_{RC}. For example, at $R=100$ kΩ, $f_{RC}=265$ Hz whereas $f_{\text{measured}}=181$ kHz because β has the very small value of 0.064. The order of the Wien oscillator in this case is 1.064, i.e. slightly higher than first-order, yet still oscillating.

DOI: 10.1002/cta

Table VII. Experimental results for the Wien oscillator of Figure 2(a).

R (kΩ)	f_{RC} (kHz)	f_{measured} (kHz)	β	Φ (deg.)		
0.2	23.42	256	0.988	42		
0.5	93.668	188	0.9003	26		
0.8	58.542	156	0.858	21		
1	46.834	136	0.844	19		
1.5	31.223	113	0.809	16		
2	23.417	98	0.785	13		
4	11.709	68	0.729	12		
8	5.854	50	0.661	8		1 cm
10	4.423	50	0.617	7		
11	4.021	51	0.6	6.5		
11.5	3.846	52	0.59	6		
13	3.402	152	0.448	0		
14	3.159	187	0.416	0		
15	2.949	205	0.397	0		
20	2.212	336	0.31	0		
30	1.474	319	0.259	0		
9	2.95	606	0.297			
30	0.885	335	0.185			
40	0.663	295	0.155		2 cm	
50	0.531	272	0.131			
100	0.265	181	0.064			

6. CONCLUSION

Four practical RC and LC oscillators were modified to include fractional-order capacitors and inductors. The general oscillation condition and oscillation frequency equations were derived, from which integer-order oscillators' design equations can be found as special cases. A clear advantage of fractional-order oscillators, which was verified experimentally, is the dependence of the oscillation frequency not only on the values of C (L) but also on the fractional order. This allows to obtain very high oscillation frequencies even if C (or L) are large. This fact may be significant enough to motivate research in hope of commercializing a fractional-order device. Sinusoidal oscillators will remain a continuously active research area of high importance [30, 31].

ACKNOWLEDGEMENTS

The authors wish to thank Eng. A. Abd Elahdi, from Sharjah University for his assistance with the lab experiments.

REFERENCES

1. Koeller RC. Applications of fractional calculus to the theory of viscoelasticity. *Journal of Applied Mechanics* 1984; **51**:299–307.
2. Matignon D, D'Andréa-Novel B. Observer based controllers for fractional differential systems. *Conference on Decision and Control SIAM*, *IEEE-CSS*, California, 1997; 4967–4972.
3. Melchior P, Orsoni B, Lavialle O, Oustaloup A. The CRONE toolbox for Matlab: fractional path planning design in robotics. *Laboratoire d'Automatique et de Productique* (LAP) 2001.

DOI: 10.1002/cta

4. Robinson DA. The use of control system analysis in neurophysiology of eye movements. *Annual Review of Neuroscience* 1981; **4**:462–503.
5. Ahmad W, El-khazali R, Elwakil AS. Fractional-order Wien-bridge oscillator. *Electronics Letters* 2001; **37**: 1110–1112.
6. Jifeng W, Yuankai L. Frequency domain analysis and applications for fractional-order control systems. *Journal of Physics*: *Conference Series* 2005; **13**:268–273.
7. Roy S. On the realization of a constant-argument immitance or fractional operator. *IEEE Transactions on Circuits and Systems* 1967; **14**:264–274.
8. Carlson G, Halijak C. Approximation of fractional capacitors $(1/s)^{1/n}$ by a regular Newton process. *IEEE Transactions on Circuits and Systems* 1964; **11**:210–213.
9. Steiglitz K. An RC impedance approximation to $s^{-1/2}$. *IEEE Transactions on Circuits and Systems* 1964; **11**:160–161.
10. Nakagawa M, Sorimachi K. Basic characteristics of a fractance device. *IEICE Transactions on Fundamentals of Electronics Communications and Computer Sciences* 1992; **E75**(12):1814–1819.
11. Saito K, Sugi M. Simulation of power-law relaxations by analog circuits: fractal distribution of relaxation times and non-integer exponents. *IEICE Transactions on Fundamentals of Electronics Communications and Computer Sciences* 1993; **E76**(2):205–209.
12. Sugi M, Hirano Y, Miura YF, Saito K. Simulation of fractal immitance by analog circuits: an approach to the optimized circuits. *IEICE Transactions on Fundamentals of Electronics Communications and Computer Sciences* 1999; **E82**(8):1627–1634.
13. Abbisso A, Caponetto R, Fortuna L, Porto D. Non-integer-order integration by using neural networks. *Proceedings of International Symposium on Circuits and Systems* 2001; **38**:688–691.
14. Arenta A, Caponetto R, Fortuna L, Porto D. Nonlinear non-integer order circuits and systems. *World Scientific Series on Nonlinear Science*, *Series A* 2002; **38**.
15. Meilanov R. Features of the phase trajectory of a fractal oscillator. *Technical Physics Letters* 2002; **28**:30–32.
16. Biswas K, Sen S, Dutta P. Modeling of a capacitive probe in a polarizable medium. *Sensors and Actuators A*: *Physical* 2005; **120**:115–122.
17. Biswas K, Sen S, Dutta P. Realization of a constant phase element and its performance study in a differentiator circuits. *IEEE Circuits and Systems II* 2006; **53**:802–806.
18. Elwakil A, Ahmed W. On the necessary and sufficient conditions for latch-up in sinusoidal oscillators. *International Journal of Electronics* 2002; **89**:197–206.
19. Matignon D. Stability results in fractional differential equation with applications to control processing. *Proceedings of Multi-conference on Computational Engineering in Systems and Application IMICS*, *IEEE-SMC*, vol. 2, France, 1996; 963–968.
20. Bonnet C, Partington J. Coprime factorizations and stability of fractional differential equations. *Systems and Control Letters* 2000; **41**:167–174.
21. Diethelm K, Ford N. Analysis of fractional differential equations. *Journal of Mathematical Analysis and Applications* 2002; **265**:229–248.
22. Pi C, Peng G. Chaos in Chen's system with a fractional order. *Chaos*, *Solitons and Fractals* 2004; **22**:443–450.
23. Radwan A, Elwakil A, Soliman A, Elsedeek A. On the stability of linear systems with fractional-order elements. *Chaos*, *Solitons and Fractals*, in press.
24. Oustaloup A. Fractional-order sinusoidal oscillators-optimization and their use in highly linear FM modulation. *IEEE Transactions on Circuits and Systems I* 1981; **28**:1007–1009.
25. Kutay M, Ozaktas H. The fractional Fourier transform and harmonic oscillations. *Nonlinear Dynamics* 2002; **29**:157–172.
26. Miller KS, Ross B. *An Introduction to the Fractional Calculus and Fractional Differential Equations*. Wiley: New York, 1993.
27. Hartley TT, Lorenzo CF. Initialization, conceptualization, and application in the generalized fractional calculus. *NASA/TP-1998-208415*, National Aeronautics and Space Administration, 1998.
28. Oldham KB, Spanier J. *Fractional Calculus*. Academic Press: New York, 1974.
29. Radwan A. Fractional-order oscillators and fractional-order filters: theories and applications. *Ph.D. Thesis*, Cairo University, December 2006.
30. Demir A. Fully nonlinear oscillator noise analysis: an oscillator with no asymptotic phase. *International Journal of Circuit Theory and Applications* 2007; **35**:175–203.
31. Souliotis G, Psychalinos C. Harmonic oscillators realized using current amplifiers and grounded capacitors. *International Journal of Circuit Theory and Applications* 2007; **35**:165–173.

DOI: 10.1002/cta